

Boger Fluid Flow through Hyperbolic Contraction Microchannels

Laura CAMPO-DEAÑO^{1,*}, Francisco J. GALINDO-ROSALES², Mónica S. N. OLIVEIRA², Manuel A. ALVES²,
Fernando T. PINHO¹

* Corresponding author: Tel.: +351 225 081 079; Fax: +351 225 081 440; Email: campo@fe.up.pt

¹ CEFT, Departamento de Engenharia Mecânica, Faculdade de Engenharia da Universidade do Porto, Portugal.

² CEFT, Departamento de Engenharia Química, Faculdade de Engenharia da Universidade do Porto, Portugal.

Abstract Boger fluids are characterized by their constant viscosity and elasticity and are very useful to study pure elastic flow behavior. In this paper we assess the potential of a microfluidic hyperbolic contraction as a device to measure the relaxation time of low viscosity polymer solutions, which are difficult to characterize in a conventional capillary break-up extensional rheometer. For this purpose we initially characterize the shear and extensional rheology of aqueous solutions of polyacrylamide (PAA) at different concentrations (400, 250, 125 and 50 ppm) with 1% (w/w) of NaCl, which result in low viscosity Boger fluids. Subsequently, flow visualizations of their flow through a microfluidic hyperbolic contraction were carried out in order to quantify the relation between their degree of elasticity and the vortex growth upstream of the microchannel.

Keywords: Boger Fluids, Rheology, Contraction-expansion flow, Relaxation time.

1. Introduction

It is well known that microfluidic devices constitute a useful alternative to study fluid flows at large deformation rates and significantly small inertial effects, characterized by low Reynolds numbers (Rodd et al., 2007).

Non-Newtonian fluid flows, in contrast to Newtonian fluid flows, show a wide range of unexpected flow features at microscale due to their strong shear-rate dependent viscosity and non-linear elastic behavior (Barnes, 2000). Additionally, at low polymer concentrations, the use of macro devices to characterize their rheology and in particular their elasticity becomes increasingly difficult due to concomitant inertial effects. Hence, characterizing the elasticity of dilute polymer solutions under extensional flows becomes a difficult task.

Boger fluids are viscoelastic fluids with shear independent viscosity and their use allows a clear separation between elastic and viscous effects (Boger, 1997). There are some studies dealing with the extensional flow of *highly*

viscous Boger fluids (Rodd et al., 2007; Rothstein and McKinley, 1998; Alves et al., 2005; Sousa et al., 2009), but few related with Boger fluids made from very low viscous solvents. However, these low viscosity elastic fluids are commonly used in microfluidic devices, and their importance is growing. Hence, it is very important to be able to characterize their rheology and to adequately assess and separate shear-thinning and elasticity effects in controlled benchmark flows.

Aitkadi et al. (1987) analyzed the effects of adding salt to aqueous solutions of polyacrylamide (PAA) and they found that it has a stabilizing effect on shear viscosity, resulting in a Boger fluid behavior. These Boger fluids are very convenient to study the extensional viscosity in microchannels without significant inertial effects.

One promising method to study extensional flows uses a microchannel with a hyperbolic contraction, which provides a quasi-uniform extensional rate at the centerline of the geometry (Oliveira et al., 2007). In this work various PAA solutions with 1% NaCl (w/w)

are rheologically characterized first in order to observe its shear and extensional flow behavior. Subsequently, flow visualizations are made with these fluids in a hyperbolic contraction micro-channel in order to determine the relaxation time of the solutions, as an alternative to the use of a capillary break-up extensional rheometer (CaBER), in which measurements of the relaxation time of dilute polymer solutions becomes particularly difficult.

2. Material and Methods

2.1 Low viscosity Boger fluids

Polyacrylamide with a molecular weight $M_w = 18 \times 10^6$ g/mol (Polysciences) was used to prepare the viscoelastic solutions by mixing the polymer into the solvent (de-ionized water) at different concentrations (50, 125, 250 and 400 ppm), using magnetic stirrers at low speeds in order to prevent mechanical degradation of the polymer. Moreover, 1% (w/w) of NaCl was added to the solutions in order to obtain low viscosity Boger fluids (solutions with nearly constant viscosity).

2.2 Rheological characterization

The fluid rheology was characterized in both extensional and shear flows. For the shear measurements, experiments were performed on a stress-controlled shear rheometer (Anton Paar, model Physica MCR301), with a plate-plate geometry of 50 mm diameter and a gap of 0.10 mm. Steady shear flow measurements in the range of shear rates, $0.1 \leq \dot{\gamma} / \text{s}^{-1} \leq 10\,000$, were carried out at various temperatures (10, 15, 20 and 25 °C). For the extensional flow, a Haake CaBER-1 extensional rheometer (Thermo Haake GmbH) was used, equipped with circular plates of 6 mm diameter, in order to follow the time evolution of the filament diameter. In the present study the initial and the final gap between plates were 3.0 and 12.03 mm, respectively. Fluid samples were carefully loaded between the plates using a syringe to ensure the absence of trapped air between the sample and the plates.

2.3 Microchannel geometry and flow visualizations

The microchannel used in this work is planar and presents a hyperbolic contraction followed by an abrupt expansion. The total width of the channel is $D_1 = 400 \mu\text{m}$, the minimum width of the contraction is $D_2 = 54 \mu\text{m}$ and the length of the hyperbolic contraction is $L_c = 126 \mu\text{m}$, resulting in a total Hencky strain of $\varepsilon_H = \ln(D_1/D_2) = 2$. The depth of the microchannel is constant, $h = 45 \mu\text{m}$. Flow visualizations were obtained using streak photography. The optical setup consists of an inverted epi-fluorescence microscope (DM IL LED, Leica Microsystems GmbH) equipped with a CCD camera (DFC350 FX, Leica Microsystems GmbH), a light source (100 W mercury lamp) and a filter cube (Leica Microsystems GmbH, excitation filter BP 530-545 nm, dichroic 565 nm and barrier filter 610-675 nm). A syringe pump (PHD2000, Harvard Apparatus) was used to inject the fluid and control the flow rate in the microchannel. Syringes with different volumes (50 μl – 100 μl) were used according to the desired flow rate and connected to the microgeometries using Tygon tubing of 0.44 mm internal diameter. The fluids were seeded with 1 μm fluorescent tracer particles (Nile Red, Molecular Probes, Invitrogen, Ex/Em: 520/580 nm) and sodium dodecyl sulfate (SDS, Sigma-Aldrich) at 0.05 wt% was added in order to minimize adhesion of fluorescent tracer particles to the channel walls. The microgeometry containing the seeded fluid was continuously illuminated and the light reflected by the fluorescent tracer particles was imaged through the microscope objective (10X, NA = 0.25) onto the CCD array of the camera using “long” exposure times (which were varied according to the flow rate) in order to capture the particles pathlines.

3. Results and Discussion

3.1 Rheological measurements

The steady shear viscosity of the four PAA solutions (400, 250, 125 and 50 ppm) was measured at different temperatures between 283.2 K and 298.2 K. Using the time-

temperature superposition principle, a master curve was obtained for each fluid at a reference temperature ($T_0 = 293.2$ K). The corresponding shift factors a_T , to make the curves overlap, are given by:

$$a_T = \frac{\eta(T)}{\eta(T_{ref})} \frac{T_{ref}}{T} \frac{\rho_{ref}}{\rho} \quad (1)$$

where $\eta(T)$ is the shear viscosity at temperature T and $\eta(T_{ref})$ and ρ_{ref} are the shear viscosity and density at the reference temperature, T_{ref} , respectively.

Figure 1 shows the viscosity master curves for the polymer solutions with and without addition of salt. In the absence of salt all solutions exhibit a significant shear-thinning behavior, which is stronger at higher concentrations. This behavior is very common with dilute polymer solutions and has been reported elsewhere (e.g. Cross, 1979, Ryder and Yeomans, 2006). Furthermore, the shear viscosity increases with increasing polymer concentration, as expected. On the other hand, the addition of NaCl reduces the shear viscosity and severely reduces its dependence on the shear rate, leading to a nearly constant shear viscosity for a wide range of shear rates. The reason for this phenomenon is the ability of the NaCl to interfere with the electronic clouds around molecules in such way that it decreases the apparent size of the PAA macromolecules and therefore reducing the molecular interactions and fluid viscosity of the PAA solutions (Ghannam, 1999).

For the PAA concentrations of 250 and 400 ppm a slight shear-thinning behavior is still present. However, for the smallest concentration, the range of measured shear rates varies from 40 s^{-1} (limit of the minimum resolution line corresponding to 10 times the minimum torque of the rheometer) to $10\,000 \text{ s}^{-1}$, where Figure 1 shows constant viscosity values. For $\dot{\gamma} < 40 \text{ s}^{-1}$ a slight shear-thinning tendency is observed but since the viscosities are below the acceptance line (marking 10 times the minimum torque) its uncertainty is large.

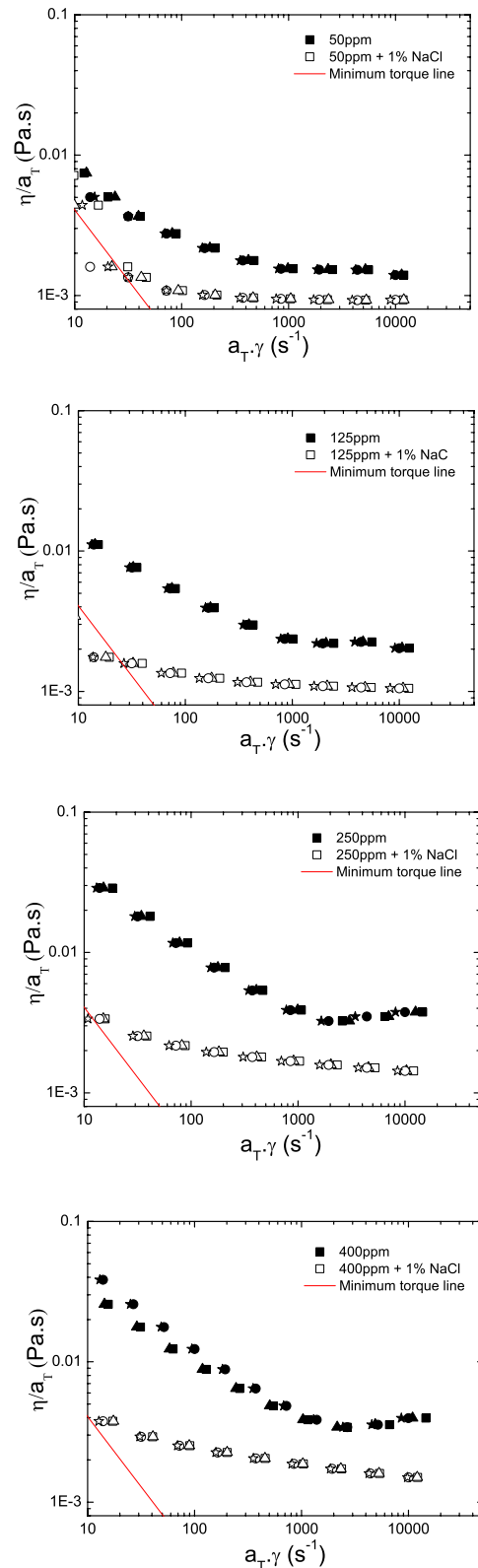


Fig. 1. Master curves of shear viscosity for PAA aqueous solutions at 50, 125, 250 and 400 ppm with and without the addition of 1% of NaCl, carried out at 283.2 (■), 288.2 (▲), 293.2 (●) and 298.2 K (*). Filled symbols represent samples without salt, and empty symbols represent samples with NaCl.

The extensional rheology of the polymer solutions with and without NaCl was evaluated using the CaBER rheometer. The relaxation time of the solutions was determined by fitting Eq. (2) to the measured data expressing the time evolution of filament diameter:

$$\frac{D_{mid}(t)}{D_0} = \left(\frac{GD_0}{4\sigma} \right)^{1/3} \exp[-t/3\lambda] \quad (2)$$

where $D_{mid}(t)$ is the time-dependent diameter filament, D_0 is the initial diameter, G is the elastic modulus of the filament, σ is the surface tension and λ is the characteristic relaxation time.

The results obtained are shown in Table 1.

Table 1

Relaxation times determined from capillary break-up experiments

Polymer concentration	No salt	1% NaCl
	λ (ms)	
400 ppm	105 ± 3	29 ± 2
250 ppm	98 ± 3	18 ± 2
125 ppm	59 ± 2	10 ± 2
50 ppm	10 ± 2	4.3 ± 0.5

The more concentrated solutions (400 and 250 ppm) have the highest relaxation times, i.e., highest elasticities. The addition of salt decreases significantly the relaxation time of the more concentrated samples, and by a lesser amount that of the 50 ppm PAA solution. The tendency is similar to the one observed for the shear viscosity value, but the degree of reduction of the relaxation time is larger in relative terms.

The extensional experiments for the lowest polymer concentrations (50 and 125 ppm) are more difficult to carry out and analyze due to their lower viscosities. The inertial instabilities lead to oscillations of the end drops together with a loss of axisymmetry and of top-bottom symmetry of the filament until the final breaking point. For that reason the experimental error associated with these measurements is higher for the less concentrated solutions (Campo-Deaño and Clasen, 2010).

3.1 Flow visualizations

In this section the flow patterns of the flow through the hyperbolic contraction/sudden expansion obtained with the Newtonian fluid (de-ionized water) and the PAA aqueous solutions with 1% of NaCl, at concentrations of 50, 125, 250 and 400 ppm respectively, are presented. The fluid flow is characterized in terms of the Reynolds and Deborah numbers, here defined according to Equations 3 and 4:

$$Re = \frac{\rho U_2 D_2}{\eta_\infty} = \frac{\rho Q}{\eta_\infty h} \quad (3)$$

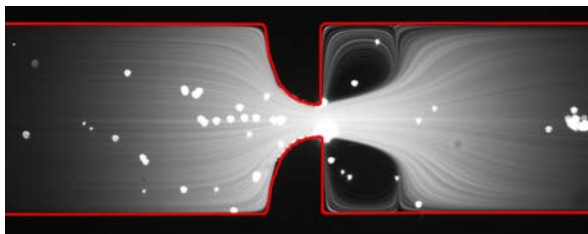
$$De = \frac{\lambda(U_2 - U_1)}{L} = \lambda \frac{Q}{hL} \left(\frac{1}{D_2} - \frac{1}{D_1} \right) \quad (4)$$

where Q is the volumetric flow rate, h is the constant depth of the microchannel, ρ is the fluid density, λ is the relaxation time and L is the length of the hyperbolic region. D_1 and D_2 are the widths of the inlet channel and throat, respectively and the characteristic viscosity is taken as the high shear rate value η_∞ obtained from rheological experiments.

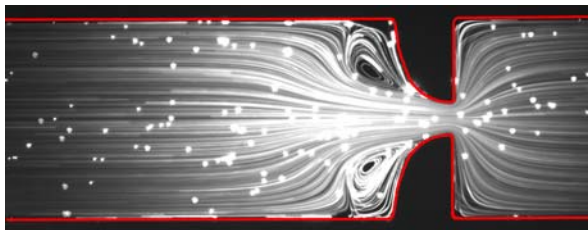
For the Newtonian fluid, the low Re flow remains symmetric about the midplane ($y = 0$) of the device and remains attached to the walls of the microchannel downstream of the hyperbolic contraction, as is the case with water at a flow rate of 1ml/h, corresponding to $Re \sim 1$, which is not shown here for compactness. When Re increases inertial effects become important and downstream lip vortices appear and are further enhanced ($Re > 30$). The recirculations grow with inertia and for $Re > 49$, they already extend to the side-walls close to the far corner, as shown in Figure 2(a). These results are in agreement with numerical simulations (Oliveira et al., 2007).

The Deborah number represents the ratio between the characteristic relaxation time of the fluid and the characteristic time of the flow and plays an important role in the characterization of the flow of viscoelastic fluids. When the flow rate is small the flow

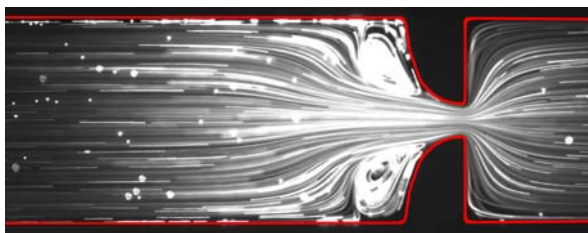
patterns are Newtonian-like (data not shown here), i.e., there is no flow separation since the Reynolds number is small. However, with an increment of the flow rate lip vortices appear upstream of the contraction. As the polymer concentration increases these vortices appear at progressively lower flow rates, corresponding to the critical values of Re and De . These differences are in accordance with the degree of elasticity, i.e., as the polymer concentration increases the fluid relaxation time also increases (cf. Table 1), therefore the elastic effects become stronger. Figure 2 shows the flow patterns for flow rate conditions above the critical value for the onset of secondary flow. For PAA concentrations from 50 to 400 ppm, the critical Reynolds number decreases by one order of magnitude whereas the critical Deborah number only changes (increases) by around 40%, and this is probably due to the different inertial levels.



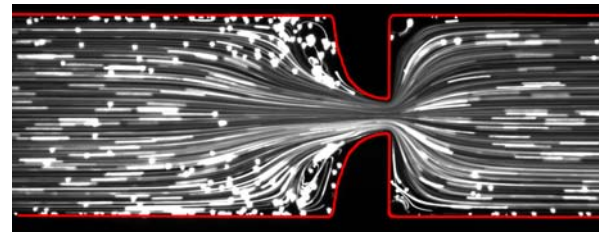
a) $Q = 15\text{ml/hr}$; $Re = 92.4$ ($\eta = 1\text{ mPa.s}$)



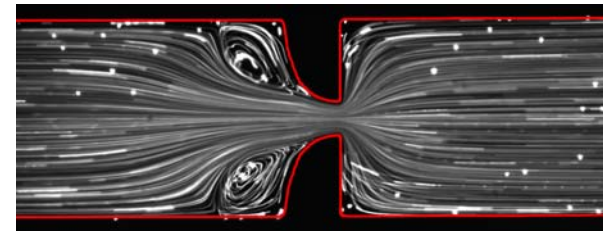
b) $Q = 1\text{ml/hr}$; $Re = 6.16$; $De = 2.98$ ($\eta_{\infty} = 1\text{ mPa.s}$)



c) $Q = 0.50\text{ml/hr}$; $Re = 2.93$; $De = 3.81$ ($\eta_{\infty} = 1.05\text{ mPa.s}$)



d) $Q = 0.30\text{ml/hr}$; $Re = 1.29$; $De = 4.26$ ($\eta_{\infty} = 1.43\text{ mPa.s}$)



e) $Q = 0.25\text{ml/hr}$; $Re = 1.03$; $De = 5.71$ ($\eta_{\infty} = 1.5\text{ mPa.s}$)

Fig. 2. Flow patterns for (a) de-ionized water and aqueous PAA solutions at (b) 50, (c) 125, (d) 250 and (e) 400 ppm, with 1% NaCl, at flow rate above the critical conditions for secondary flow. The flow direction is from left to right.

If the Deborah number further increases the vortex size also increases due to the progressive enhancement of elastic effect, eventually leading to an unsteady asymmetric separated flow as, for instance, with the 400 ppm solution at a flow rate of 1 ml/h, not shown for conciseness. The growth of the vortex size is here characterized in terms of the dimensionless vortex length, $X_R = L_v/D_1$ (where L_v is the vortex length along the stream wise direction and D_1 is the upstream channel width).

The evolution of the normalized vortex length with De is shown in Figure 3 for the four polymer solutions with salt. The curve for all polymer solutions follows approximately the same trend (taking into account the experimental uncertainty, showed as horizontal error bars, calculated from the experimental uncertainty of the relaxation time measurements), which represents a quasi-linear relationship between X_R and De . At high De the slope decreases slightly, especially for the less concentrated solutions. In particular, for the 50 ppm PAA solution at high De a different trend can be observed, presumably

related to the fact that for the less concentrated polymer solutions the Reynolds number becomes important as the flow rate and consequently (De) increases and the effect of inertia opposes that of elasticity in terms of the length of the upstream vortices.

Inspired by the data of Figure 3, and in particular by the small variation of the critical value of De , it is possible to propose a new approach able to provide a reliable indirect measurement of the relaxation time for polymer solutions at low concentration, which can be used together with measurements obtained by the CaBER system. It consists of an extrapolation from the relaxation time obtained for the highest concentrations (400 and 250 ppm) to the lowest concentration (50 ppm), assuming that the critical De is essentially independent of the polymer concentration. In this particular case, where the critical Deborah number is $De_{cr} \approx 4.5$ by using Equation 4, we can estimate the relaxation time for the 50 ppm solution to be $\lambda \approx 5$ ms, which is in good agreement with the CaBER measurement value, despite the inherent difficulties in this measurement.

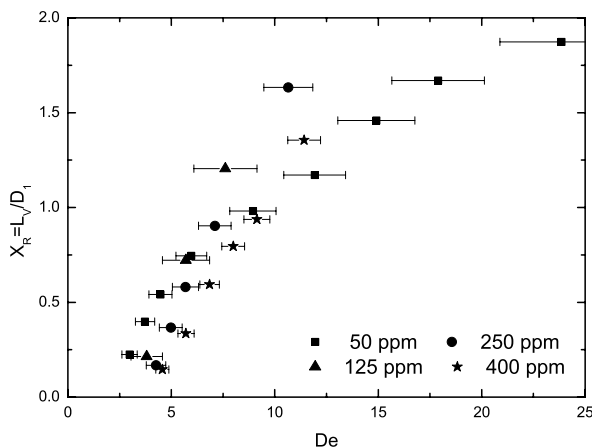


Fig. 3. Effect of Deborah number on the dimensionless vortex length in the steady symmetric regime for the 50, 125, 250 and 400 ppm PAA aqueous solutions with salt.

4. Conclusions

In this paper the shear and extensional flow behavior of aqueous solutions of PAA at weight concentrations of 50, 125, 250 and 400 ppm were carried out. It was shown that the

addition of 1% of NaCl to these polymer solutions changed their rheological properties, resulting in a nearly constant viscosity elastic fluid. These Boger fluids are very useful to study elastic effects in microfluidic devices, due to the negligible influence of inertial and shear-thinning effects. Subsequently, flow visualizations through the planar geometry containing an hyperbolic contraction followed by an abrupt expansion, allowed us to propose a new method for the determination of relaxation times of low viscosity dilute polymer solutions based on the quantification of the vortex growth upstream of the hyperbolic contractions and the fact that the onset of this critical Deborah number varies weakly with the polymer concentration for a particular set of polymer solutions. This method can be used in conjunction with CaBER measurements for more concentrated solutions and provides reliable results at low polymer concentration.

Acknowledgements

Authors acknowledge funding from Fundação para a Ciência e a Tecnologia (FCT), COMPETE and FEDER through projects PTDC/EQU-FTT/ 71800/2006, PTDC/EQU-FTT/70727/2006, PTDC/EME-MFE/099109/2008, REEQ/928/EME/2005 and REEQ/298/EME/2005. F.J. Galindo-Rosales acknowledges FCT for financial support (scholarship SFRH/BPD/69663/2010).

References

- Aitkadi, A., Carreau, P., Chauveteau, G. 1987. Rheological properties of partially hydrolyzed polyacrylamide solutions. *Journal of Rheology* 31, 537–561.
- Alves, M. A., Pinho, F. T., Oliveira, P. J. 2005. Visualizations of Boger fluid flows in a 4:1 square-square contraction. *AIChE Journal* 51, 2908–2922.

Barnes, H. A., 2000. A Handbook of Elementary Rheology, Institute of Non-Newtonian Fluid Mechanics, University of Wales, Aberystwyth, Wales.

Boger, D. V., 1997. A highly elastic constant-viscosity fluid. *Journal of Non-Newtonian Fluid Mechanics* 3, 87–91.

Campo-Deano, L., Clasen, C. 2010. The slow retraction method (SRM) for the determination of ultra-short relaxation times in capillary break-up extensional rheometry experiments. *Journal of Non-Newtonian Fluid Mechanics* 165,1688–1699.

Cross, M. M., 1979. Relation between viscoelasticity and shear-thinning behavior in liquids. *Rheologica Acta* 18, 609–614.

Ghannam, M. T. 1999. Rheological properties of aqueous polyacrylamide / NaCl solutions. *Journal of Applied Polymer Science* 72, 1905–1912.

Oliveira, M. S. N., Alves, M. A. , Pinho, F. T., McKinley, G. H. 2007. Viscous flow through microfabricated hyperbolic contractions. *Experimental Fluids* 43, 437–451.

Ryder, J. F., Yeomans, J. M. 2006. Shear thinning in dilute polymer solutions, *Journal of Chemical Physics* 125, 194906.

Rodd, L. E., Cooper-White, J. J., Boger, D. V., McKinley, G. H., 2007. Role of the elasticity number in the entry flow of dilute polymer solutions in micro-fabricated contraction geometries. *Journal of Non-Newtonian Fluid Mechanics* 143, 170–191.

Rothstein, J. P., McKinley, G. H. 1998. Extensional flow of a polystyrene Boger fluid through a 4:1:4 axisymmetric contraction/expansion. *Journal of Non-Newtonian Fluid Mechanics* 86, 61–88.

Sousa, P. C., Coelho, P. M., Oliveira, M. S. N. Alves, M. A. 2009. Three dimensional flow of Newtonian and Boger fluids in square-square

contractions. *Journal of Non-Newtonian Fluid Mechanics* 160, 122–139.